Deep-Sea Research I 75 (2013) 52–66

Contents lists available at SciVerse ScienceDirect

Deep-Sea Research I

journal homepage: www.elsevier.com/locate/dsri

Primary production export flux in Marguerite Bay (Antarctic Peninsula): Linking upper water-column production to sediment trap flux

Keith Weston [a,b,*], Timothy D. Jickells [a], Damien S. Carson [c], Andrew Clarke [d], Michael P. Meredith [d], Mark A. Brandon [e], Margaret I. Wallace [d,e,1], Simon J. Ussher [f,2], Katharine R. Hendry [g,3]

[a] Laboratory of Global Marine and Atmospheric Chemistry, School of Environmental Sciences, University of East Anglia, Norwich NR4 7TJ, UK
[b] Centre for Environment, Aquaculture and Fisheries Science, Lowestoft, Suffolk NR33 0HT, UK
[c] School of GeoSciences, The University of Edinburgh, West Mains Road, Edinburgh EH9 3JW, UK
[d] British Antarctic Survey, NERC, High Cross, Madingley Road, Cambridge CB3 0ET, UK
[e] Earth and Environmental Sciences, The Open University, Walton Hall, Milton Keynes MK7 6AA, UK
[f] School of Geography, Earth and Environmental Science, University of Plymouth, Plymouth PL4 8AA, UK
[g] Department of Earth Sciences, University of Oxford, South Parks Road, Oxford OX1 3AN, UK

ARTICLE INFO

Article history:
Received 16 May 2012
Received in revised form
29 January 2013
Accepted 7 February 2013
Available online 14 February 2013

Keywords:
Primary production
New production
Regenerated production
f ratio
Antarctic Peninsula
Southern Ocean

ABSTRACT

A study was carried out to assess primary production and associated export flux in the coastal waters of the western Antarctic Peninsula at an oceanographic time-series site. New, i.e., exportable, primary production in the upper water-column was estimated in two ways; by nutrient deficit measurements, and by primary production rate measurements using separate ^{14}C-labelled radioisotope and ^{15}N-labelled stable isotope uptake incubations. The resulting average annual exportable primary production estimates at the time-series site from nutrient deficit and primary production rates were 13 and 16 mol C m^{-2}, respectively. Regenerated primary production was measured using ^{15}N-labelled ammonium and urea uptake, and was low throughout the sampling period.

The exportable primary production measurements were compared with sediment trap flux measurements from 2 locations; the time-series site and at a site 40 km away in deeper water. Results showed ~1% of the upper mixed layer exportable primary production was exported to traps at 200 m depth at the time-series site (total water column depth 520 m). The maximum particle flux rate to sediment traps at the deeper offshore site (total water column depth 820 m) was lower than the flux at the coastal time-series site. Flux of particulate organic carbon was similar throughout the spring–summer high flux period for both sites. Remineralisation of particulate organic matter predominantly occurred in the upper water-column (< 200 m depth), with minimal remineralisation below 200 m, at both sites. This highly productive region on the Western Antarctic Peninsula is therefore best characterised as 'high recycling, low export'.

1. Introduction

Biogeochemical processes in Antarctic coastal waters can exert important influences on both benthic and planktonic ecological phenomena, e.g., Karl et al. (1991), Barnes and Clarke (1994), Prezelin et al. (2000), Smith et al. (2008). These processes also have the potential to exert larger scale impacts on the chemistry of the globally important water masses that form on the Antarctic shelf (Broecker and Peng, 1982; Falkowski et al., 1998).

The short phytoplankton production season drives many of the biogeochemical processes involved (Clarke et al., 2008; Ducklow et al., 2008). Despite a short phytoplankton growth period in these Antarctic shelf regions, the overall annual primary productivity is high relative to the Southern Ocean (Arrigo et al., 1998; Vernet et al., 2008). This is in part due to the presence of sufficient trace nutrients, e.g., dissolved Fe, in coastal Antarctic waters (Ardelan et al., 2010) in contrast to the Southern Ocean (Martin et al., 1990).

This high primary production can however only be exported if it is in part 'new' production (*sensu* Dugdale and Goering, 1967). In order to calculate this 'new' or exportable primary production, concurrent measurements of rates of new, regenerated and total primary production were carried out at the Rothera Oceanographic and

* Corresponding author at: University of East Anglia, School of Environmental Sciences, Laboratory of Global Marine and Atmospheric Chemistry, Norwich NR4 7TJ, UK. Tel.: +44 1502 524210; fax: +44 1502 513865.
E-mail address: keith.weston@cefas.co.uk (K. Weston).
[1] *Present address:* Scottish Environment Protection Agency, Bremner House, The Castle Business Park, Stirling FK9 4 TF, UK.
[2] *Present address:* Bermuda Institute of Ocean Sciences, Ferry Reach, St. Georges GE01, Bermuda.
[3] *Present address:* School of Earth and Ocean Sciences, Cardiff University, Main Building, Park Place, Cardiff CF10 3AT, UK.

0967-0637/$ - see front matter © 2013 Elsevier Ltd. All rights reserved.
http://dx.doi.org/10.1016/j.dsr.2013.02.001

Biological Time Series (RaTS) site in Marguerite Bay. The RaTS was initiated at this site in 1997 to investigate the impacts of climatic change on the physical, biogeochemical and biological aspects of the Antarctic marine environment (Clarke et al., 2008). Climate change is particularly pronounced in polar regions because of the number of feedbacks in the ice–atmosphere–ocean system (Smith et al., 1998; Meredith and King, 2005; Clarke et al., 2007; Montes-Hugo et al., 2009). Concurrent estimates of new primary production from nutrient profiles were also carried out using the approach of Serebrennikova and Fanning (2004). Combining the short-term direct rate measurements of phytoplankton growth with the nutrient drawdown method, which integrates to some extent over space and time, allows an improved estimation of the areal annual exportable primary production for the Marguerite Bay region.

The exportable primary production in the upper water-column may in turn result in export of organic matter to deeper waters, if it is not remineralised during export. The primary production that is exported is important both for understanding C and other macronutrient cycles, and for the delivery organic material to support benthic faunal communities (Smith et al., 2008). In order to quantify this exported flux, there have been many studies using sediment traps along the Antarctic Peninsula, e.g., von Bodungen et al. (1986), Palanques et al. (2002), Baldwin and Smith (2003), Kim et al. (2004). The introduction of sediment trapping studies lasting many years on the WAP has in particular highlighted the extreme annual variability of these fluxes and high flux rates during summer (Ducklow et al., 2007). In the southern region of the western Antarctic Peninsula (WAP), diatom dominance of summer primary production (Huang et al., 2012) may result in higher rates of biogenic opal flux to deep water (Nelson et al., 1996; Pondaven et al., 2000), in addition to delivering organic matter to the benthos (Smith et al., 2008). The deployment of sediment traps at 2 sites in this study provides the most southerly export flux measurement for the WAP. The data from the sediment traps are used to investigate how upper water-column exportable primary production (<100 m) relates to exported particle flux to deeper waters.

Overall this study constructs an annual upper water-column primary production budget at the RaTS site. This budget is then compared to nutrient drawdown-derived primary production, and particle export measurements for Marguerite Bay. The work presented here tests whether Antarctic coastal waters in the southern WAP act as a globally important CO_2 sink, as postulated by Arrigo et al. (2008a), due to high primary productivity resulting in high export flux to the benthos.

2. Methods and materials

2.1. Study sites

Marguerite Bay is a fjordic region with relatively slow water advection compared to biogeochemical process rates, making the region suitable for biogeochemical budgeting (Fig. 1a). The RaTS site is ~4 km offshore in Ryder Bay (Fig. 1b) over a water depth of 520 m (Clarke et al., 2008). This site was the location for the collection of conductivity-temperature-depth (CTD) profiles and water samples for primary production and nutrient uptake experiments (Table 1). When the main RaTS site could not be reached a secondary station was used (Fig. 1b) as in Clarke et al. (2008) and Venables et al. (In press). The secondary site is assumed to be representative of the main RaTS site, consistent with various considerations of the physical and biogeochemical system (Clarke et al., 2008; Meredith et al., 2008, 2010).

Two sediment traps and hydrographic moorings were deployed in Marguerite Bay from RRS James Clark Ross. Three successive mooring deployments were completed at the RaTS site (see Table 2). The second mooring was deployed 40 km away in an extension of the Marguerite Trough (MT site) in 820 m of water (Fig. 1a) but was lost during the second deployment (Table 2).

Marguerite Bay is located on the WAP shelf, with the Antarctic Circumpolar Current (ACC) immediately adjacent to the shelf break. This puts the WAP in an unusual oceanographic position compared with other Antarctic shelf regions, which are typically separated from the ACC by subpolar gyres that inhibit the exchange of water mass properties. The WAP's proximity to the ACC allows warm and saline Circumpolar Deep Water (CDW) from the ACC to enter onto the continental shelf along the glacially scoured troughs dissecting the shelf (Klinck et al., 2004; Martinson et al., 2008).

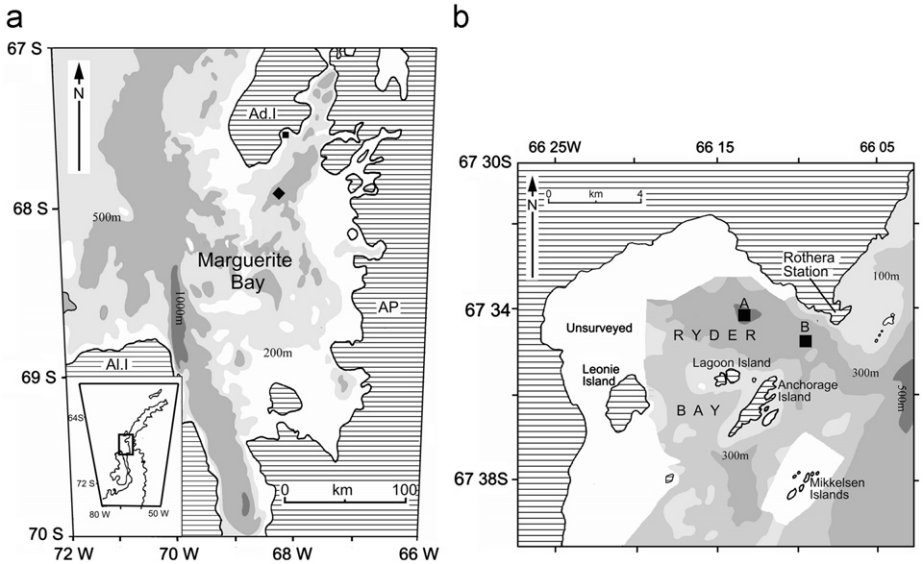

Fig. 1. (a) Location of Marguerite Bay in relation to the Western Antarctic Peninsula with Adelaide Island (Ad. I), Alexander Island (Al. I.) and the Antarctic Peninsula (AP) labelled. Depth contours of 200 m, 500 m and 1000 m shown. The locations of the RaTS and Marguerite Trough moorings are shown with square (■) and diamond (♦) symbols. (b) shows the area of Ryder Bay. The locations of the main RaTS site and the secondary RaTS site are shown by squares (■) labelled A and B, respectively. Depth contours of 100, 300 and 500 m shown.

Table 1
Comparison of sampling depth and timing, and parameters sampled during the RaTS long-term time series and in this study.

Sampling programme	Timing (Date *dd/mm/yy*)	Chlorophyll *a* (sampling depths (m)	Profile for fluorescence and temperature	Dissolved nitrate (sampling depths (m)	Dissolved ammonium (sampling depths (m)	Dissolved urea (sampling depths (m)	Total dissolvable iron (sampling depths (m)	^{15}N uptake incubations (sampling depths (m)	^{14}C uptake incubations (sampling depths (m)	Sediment flux
RaTS[a]	~Weekly (Ongoing from 1992)	Y (15 m)	Y	Y (15 m)	Y (15 m)	N	N	N	N	N
This study	Day 362 (*28/12/05*)	Y (15 m)	Y	Y (15 m)	Y (15 m)	Y (15 m)	Y (15 m)	Y (15 m)	Y (15 m)	Y
This study	Days 369–375 (*04/01/06-10/01/06*)	Y (15 m)	Y	Y (0 m, 10 m and15 m)	Y (0 m, 10 m and15 m)	Y (0 m, 10 m and15 m)	Y (15 m)	Y (0 m, 10 m and15 m)	Y (15 m)	Y
This study	Days 378–416 (*13/01/06–20/02/06*)	Y (15 m)	Y	Y (0 m, 5 m, 10 m and15 m)	Y (0 m, 5 m, 10 m and15 m)	Y (0 m, 5 m, 10 m and15 m)	Y[b] (15 m)	Y (0 m, 5 m, 10 m and15 m)	Y (15 m)	Y

[a] See Clarke et al. (2008) for full range of parameters sampled during RaTS programme.
[b] Total dissolvable iron was sampled for until day 398.

Table 2
Timings of the moorings deployments.

Mooring	No.	Location	Upper trap depth (m)	Lower trap depth (m)	Date deployed dd/mm/yy (day number)	Date recovered dd/mm/yy (day number)	Duration of deployment (days)
RaTS	1	67°34.02′S, 68°14.02′W	200	420	25/1/05 (25)	15/02/06 (411)	387
	2	67°33.97′S, 68°14.06′W	200	420	17/02/06 (413)	16/12/06 (715)	303
	3	67°34.01′S, 68°14.00′W	200	420	17/12/06 (716)	09/04/07 (829)	114
MT	1	67°55.39′S, 68°24.15′W	123[a]	735	24/01/05 (24)	15/02/06 (411)	388

[a] Upper trap depth unintentionally differed between MT and RaTS sites resulting in a shallower upper trap depth at MT than intended.

Table 3
Estimates of exportable production from upper water-column nutrient deficit calculations and rate measurements.

Site	Day number	Integrated summer nitrate (mol m^{-2})	Integrated winter nitrate (mol m^{-2})	Summer nitrate drawdown (mol m^{-2})	Nutrient deficit derived exportable production (mol C m^{-2} y^{-1})	Rate measurement derived exportable production (mol C m^{-2} y^{-1})
RaTS	25	1.4	3.8	2.4	15.9	–
	411	2.2	3.8	1.6	10.6	–
	716	2.0	3.8	1.8	11.9	–
	N/A	–	–	–	–	16.0
MT[a]	24	3.6	3.8	0.2	1.3	–
	411	2.1	3.8	1.7	11.3	–
	715	1.9	3.8	1.9	12.6	–

[a] The drawdown of nitrogen on day 829 was not used as a nutrient depleted upper mixed layer was not well defined from profile data.

The Antarctic Peninsula Coastal Current (APCC) flows southward along the western sides of Adelaide Island and Alexander Island (Moffat et al. (2008); Fig. 1a). Within Marguerite Bay there is a generally cyclonic flow connected to the boundary currents adjacent to Adelaide and Alexander Islands (Beardsley et al., 2004; Klinck et al., 2004). This potential connectivity has been used to argue that the marine system at the RaTS site is broadly representative of at least the inner part of the WAP shelf (Meredith et al., 2004), albeit with higher levels of chlorophyll *a* (chl *a*) compared to the WAP shelf as a whole (Montes-Hugo et al., 2008). Although the path of the APCC within Ryder Bay is not well understood, the hydrography at the RaTS site is characteristic of waters inshore of the westernmost edge of the APCC (Meredith et al., 2004; Moffat et al., 2008; Wallace, 2008).

2.2. Hydrography, water column macronutrient profiles and nutrient deficit-derived production

Samples were taken for dissolved nitrate and silicate profiles at up to 12 depths during the sediment trap deployment/recovery cruises on a large research vessel at both the RaTS and MT sites (Table 2) using an array of 10 l Niskin bottles attached to a rosette multisampler. A SeaBird 911plus CTD system was deployed on the same frame, with derived salinity calibrated with discrete

water samples analysed on a Guildline 8400B salinometer. Water samples for nitrate and nitrite (hereafter nitrate) were filtered through ~0.7 μm pore size pre-ashed (4 h, 400 °C) glass fibre (GF/F) filters (Whatman). Samples for macronutrients were stored frozen at −20 °C until analysis, and analysed using a Skalar autoanalyser according to Kirkwood (1996). Accuracy of nitrate and silicate analyses was confirmed by standard reference materials, with a < 5% error for analyses relative to Ocean Scientific International Ltd. (UK) standards. The detection limit for autoanalyser measurements of nitrate and silicate analyses was 0.1 μM.

The water column nutrient profiles were used to derive exportable primary production by nutrient deficit. Using this method, the difference between water-column integrated nitrate for the upper 100 m for winter and summer sampling was calculated i.e., summer nitrate drawdown (Table 3). Depth-integrated winter total (to 100 m depth) was calculated using 38 mmol m^{-3} from 0 m to 100 m. This is the average NO_3^- concentration for all depths and all CTD profiles from 200 m to bottom (see Figs. 2 and 3). The difference between integrated winter nitrate and integrated summer nitrate is assumed to arise from net nutrient uptake by phytoplankton. Summer nitrate drawdown was converted to particulate organic carbon (POC) by assuming a Redfield C/N ratio of 106:16, to estimate nutrient deficit-derived exportable primary production (Serebrennikova and Fanning, 2004). The interpretation of this calculation is relatively simple in this region since there is no N_2 fixation in this region (Karl et al., 2002), no significant riverine and atmospheric N input, and restricted access to the open ocean.

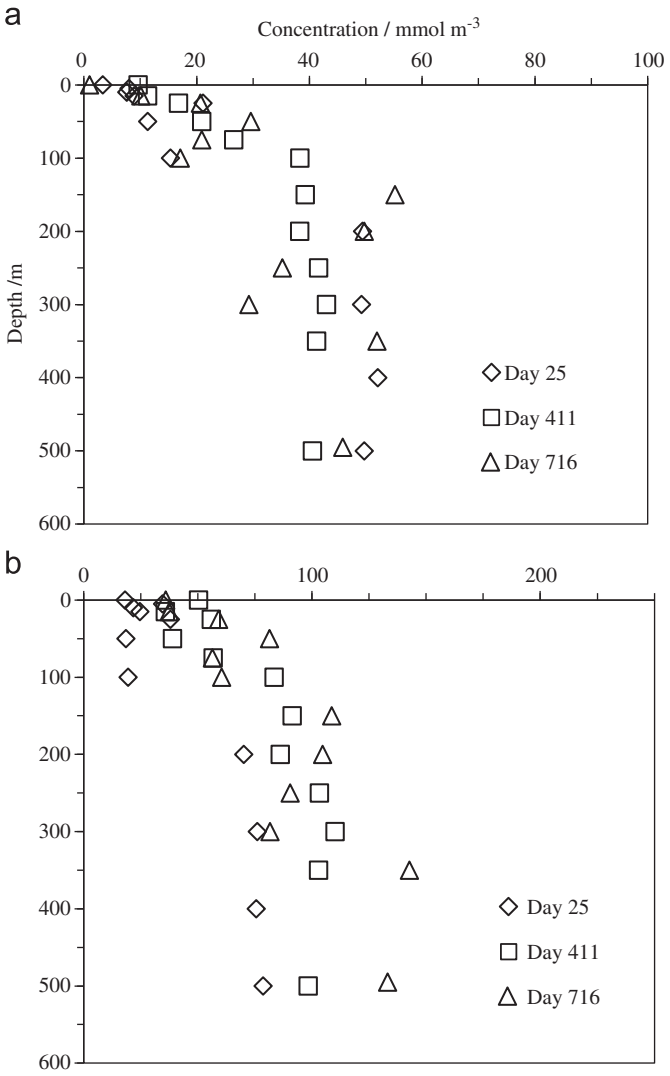

Fig. 2. Water column profiles for dissolved (a) nitrate, and (b) silicate at the RaTS site. Day 25 is 25th January 2005; day 411 is 15th February 2006; day 716 is 17th December 2006.

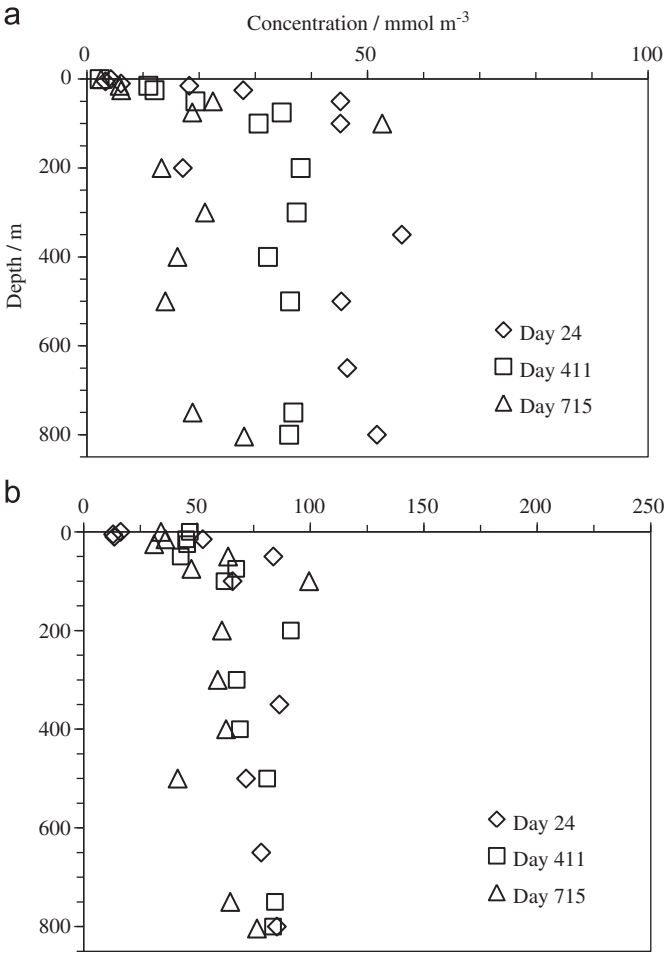

Fig. 3. Water column profiles for dissolved (a) nitrate and (b) silicate at the MT site. Day 24 is 24th January 2005; day 411 is 15th February 2006; day 715 is 16th December 2006.

2.3. Upper water-column sampling at the RaTS site

At the RaTS site biogeochemical parameters and physical oceanographic data have been collected ~weekly at 15 m depth since 1998 using a rigid inflatable boat (see Clarke et al., 2008) for a full description of the data set). During the study period physical oceanographic profiles were collected to > 500 m depth using a SeaBird SBE19+ CTD, WetLabs fluorometer and LiCor Photosynthetically Active Radiation (PAR) sensor. RaTS site salinity data were calibrated annually with SeaBird 911+ instruments carried aboard RRS James Clark Ross and ARSV L.M. Gould, themselves calibrated against P-series standard seawater.

In this study a series of additional sampling trips were made during the summer of 2005–2006 at the RaTS site only, in order to measure primary production rates at high frequency throughout one spring–summer bloom. The parameters, depths and dates sampled in this study, in comparison with the RaTS time-series sampling, are shown in Table 1.

2.3.1. Chlorophyll, trace- and macronutrient analysis

As part of the RaTS time-series, chl *a* samples from 15 m were filtered into 4 size fractions (Clarke et al., 2008). Analysis was by methanol/chloroform extraction followed by fluorometric detection (Clarke et al., 2008). The summed chl *a* for the 4 size fractions represents total chl *a* at 15 m, and was used to calibrate the chl *a* depth profile from the profile data (Clarke et al., 2008).

Samples for urea, nitrate, silicate and phosphate were filtered in the laboratory through ~0.7 μm pore size pre-ashed (4 h, 400 °C) GF/F filters. Ammonium samples were not filtered prior to analysis. Samples for urea and ammonium were analysed in triplicate immediately upon return to the laboratory. Ammonium was analysed fluorometrically according to Holmes et al. (1999) with a detection limit of 0.01 μM. Urea was analysed spectrophotometrically according to Mulvenna and Savidge (1992) with a detection limit of 0.1 μM. Samples for nitrate, silicate and phosphate were stored and analysed as for the full depth macronutrient profiles; phosphate was also analysed using a Skalar autoanalyser according to Kirkwood (1996). The detection limit for phosphate analysis was 0.2 μM. The percent error for all nutrient analyses was $<5\%$ relative to Ocean Scientific International Ltd. standards.

Sampling for total dissolvable iron (TDFe) analysis was based on Jickells et al. (2008). Water samples were collected directly with an acid-washed polypropylene syringe deployed with a weighted polypropylene line. In order to minimise blanks, samples were transferred unfiltered into a trace metal cleaned storage tube in a laminar flow hood. Samples were stored frozen at −20 °C until analysis. All analyses and subsequent sample handling were conducted in an accredited (ISO9001:2000) clean room. A month prior to analyses, samples were thawed and transferred unfiltered into a trace metal cleaned PTFE storage tube in a laminar flow hood. The samples were then acidified to pH 1.9 by addition of high purity HCl (ultrapure grade, Romil). Acidification makes some of the particulate iron available to the analytical method, in addition to the dissolved Fe. Results are therefore presented as TDFe. TDFe was determined using flow injection chemiluminescence using luminol reagent with no added oxidant following a 12 h sulphite reduction step according to Bowie et al. (1998).

2.3.2. Primary production measurements using radioisotope (^{14}C) uptake

For primary production measurements one bulk sample for ^{14}C uptake measurement was collected at 15 m. Photosynthetic uptake was measured by incubating 24 × 5 ml seawater subsamples, each spiked with 0.185 MBq of ^{14}C-labelled sodium bicarbonate solution (Amersham, UK). Subsamples were incubated for 1 h under a range of light intensities (1–2000 μmol photons $m^{-2}\,s^{-1}$) using a photosynthetron (Lewis and Smith, 1983) at surface water temperature. After incubation the samples were left unfiltered, and 375 μl of 6 M HCl added to each vial to sparge all unfixed ^{14}C. Twelve hour after acidification, all samples were fixed with 100 μl of ethanolamine. Activities of these samples were determined by liquid scintillation analysis. TCO_2 was derived using the CO_2 SYS programme (Lewis and Wallace, 1998) using alkalinity determined by titration of a water sample from 15 m depth (Almgren et al., 1983). Primary production uptake rates were calculated according to Peterson (1980).

Photosynthesis versus irradiance curves were fitted to ^{14}C uptake data by nonlinear regression according to Platt et al. (1980). This curve was then used to calculate daily water-column integrated primary production results according to Walsby (1997). This involved the calculation of maximum photosynthetic rate (P_m, or P_s under conditions of photoinhibition; mg C $m^{-3}\,h^{-1}$), the negative slope of the curve at high irradiance (β; mg C $m^{-3}\,h^{-1}$ (μmol photons $m^{-2}\,s^{-1})^{-1}$) and the gradient of the photosynthesis vs. irradiance curve (α; mg C $m^{-3}\,h^{-1}$ (μmol photons $m^{-2}\,s^{-1})^{-1}$) from the ^{14}C uptake incubations. These parameters were normalised to the chlorophyll concentration at 15 m. Primary production throughout the water column was estimated by relating these values of chlorophyll concentration at 15 m to the calibrated fluorescence at 1 m depth intervals. Production (P) was calculated using the equation of Platt et al. (1980): $P=P_s(1-e^{-\alpha I/Ps})e^{-\beta I/Ps}$, where I is in situ irradiance. PAR down the water column was then calculated according to Walsby (1997), using incident broadband PAR from Anchorage Island (Fig. 1b) with only wind speed omitted. Spreadsheets used for calculation of daily water-column integrated primary production according to Walsby (1997) can be downloaded from http://www.bristol.ac.uk/biology/research/plant/microbial/integral.html.

Daily water-column integrated production was calculated to the depth of Net Photocompensation Irradiance (NPI). The NPI depths used are shown in Table 4. NPI is the value of PAR which results in a net phytoplankton growth rate of zero, in the presence of most naturally occurring losses. These losses include respiration, grazing and release of dissolved organic carbon (Nelson and Smith, 1991). As per Boyd et al. (1995) and Clarke et al. (2008), NPI was used due to the extreme seasonality of photoperiod and irradiance flux at high latitudes, together with the confounding effect of surface ice and surficial snow. An NPI of 15 μE $m^{-2}\,s^{-1}$ was used based on measurements made in the Bellingshausen Sea (Boyd et al., 1995).

2.3.3. Stable isotope (^{15}N) uptake measurements and rate measurement-derived new production

For measurements of nitrate, ammonium and urea uptake rates, 200 ml seawater samples from a range of depths (Table 1) were transferred to 250 ml acid-washed polycarbonate flasks and spiked with either ^{15}N-sodium nitrate (99 atom percent: Isotec, USA), ^{15}N-ammonium sulphate (98 atom percent: Isotec, USA) or ^{15}N-urea (99 atom percent: Isotec, USA). All samples were enriched by an estimated 10% of in situ nutrient concentration, subject to a minimum addition of 0.02 μmol N. One sample for nitrate, ammonium and urea uptake from each depth was then filtered as a zero-time control. All other samples were incubated in triplicate for 3 h at surface seawater temperature. Incubator light levels were adjusted using neutral density filters (Lee, UK) to the sample depth irradiance (± 5% surface irradiance) according to light profiles taken during sampling. After incubation, samples were filtered onto pre-ashed (4 h, 400 °C) GF/F filters at low vacuum (< 15 mmHg). All filters were then dried (16 h, 40 °C)

Table 4
f ratio and depths of the Net Photocompensation Irradiance (NPI) and ^{15}N uptake integration.

Date (dd/mm/yy)	Day number	*f* ratio	NPI depth (m)	Depth of ^{15}N integration
28/12/05	362	0.79[a]	11	–
04/01/06	369	0.78	11	15
06/01/06	371	0.88	11	15
10/01/06	375	0.84	8	15
13/01/06	378	–[b]	9	10
19/01/06	384	0.82	9	10
24/01/06	389	0.77	10	10
30/01/06	395	0.71	10	10
02/02/06	398	0.72	8	10
13/02/06	409	0.80	7	10
20/02/06	416	0.86	6	5

[a] For 28/12/05 only 15 m depth was sampled so *f* ratio calculated from this depth only.
[b] Nitrate uptake measurement samples were lost on this sampling date.

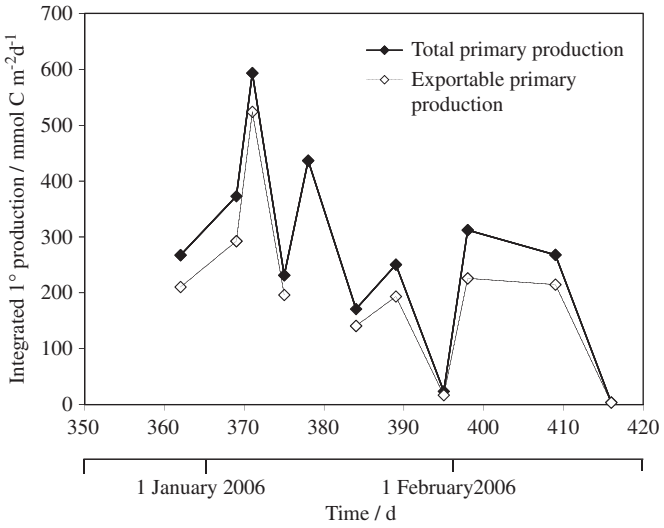

Fig. 4. Water-column integrated primary production to the depth of the Net Photocompensation Irradiance (NPI; see Table 4) at the RaTS site. Exportable primary production is the total primary production multiplied by the corresponding *f* ratio (see Table 4). Day 365 is 1st January 2006.

and stored at room temperature. Filtrate particulate N and atom percent N was determined using a Europa Scientific (UK) 20–20 continuous flow isotope mass spectrometer online with an ANCA elemental analyser. Nitrogen uptake rates were calculated using the models of Dugdale and Goering (1967). Water-column integrated N uptake was calculated using planimetric integration to a similar depth as used for water-column integrated total (^{14}C-derived) uptake measurements (see Table 4).

Exportable or 'new' primary production from rate measurements were calculated as in Weston et al. (2005) by multiplying the ^{14}C derived primary production rate by the ratio of water-column integrated nitrate uptake to the sum of the water-column integrated nitrate, ammonium and urea uptake rates, i.e., the *f* ratio (Table 4). The annual rate measurement derived exportable production (Table 3) was calculated using an average bloom length of 75 days (Clarke et al., 2008) in combination with average water-column integrated C uptake (266 mmolC m^{-2} d^{-1}; Fig. 4) and the average *f* ratio (0.8; Table 4). This 75 day period essentially represents the annual growth period, since growth is minimal outside the bloom period (Clarke et al., 2008).

2.4. Sediment flux traps

2.4.1. Sediment trap preparation and deployment

Two mooring arrays were deployed (Table 2), each consisting of two time-series sediment traps (McLane, USA), along with physical oceanography-related instrumentation (Wallace et al., 2008). Each sediment trap had 21 acid-cleaned 250 ml HDPE bottles programmed to rotate at predefined intervals.

Sediment trap preparation and analyses were consistent with the US Joint Global Ocean Flux Study (JGOFS) protocol (JGOFS, 1994). Before trap deployment, the sampling bottles were rinsed and filled with buffered filtered (0.8 μm pore size) seawater. This seawater density was increased by the addition of 5 g NaCl l^{-1}. Sodium tetraborate-buffered formalin solution was added to the sampling bottles to a concentration of 2% v/v as a preservative. The final pH of the buffered seawater was 8.0. After recovery, the supernatant from the bottle was siphoned off and analysed for dissolved nitrate and silicate according to Kirkwood (1996) using a Skalar autoanalyser as for the water-column macronutrient measurements. There was no significant loss of nitrogen or silicate to the supernatant ($<0.1\%$ relative to total sediment particulate N and opal; results not shown). Swimmers, i.e., all large zooplankton, were removed from sediment samples using plastic forceps by visually inspecting the sample with a binocular light microscope ($\times 20$ magnification). Where there was sufficient sample, the sediment was then split into 10 equal fractions using a rotary splitter.

Results from bottles open during trap recovery are not presented because they are perturbed by the recovery. Annual fluxes are therefore an underestimate. However, the timing of the bottle rotation in the sediment trap was set to reduce loss of flux due to recovery, with bottles sampling during recovery in spring/summer having sampled for a maximum of 7 days prior to trap recovery.

2.4.2. Sediment trap analysis

To determine the dry mass of trapped material, either the whole sample or a subsample was filtered onto a preweighed polycarbonate filter and rinsed with buffered (pH 8–8.5) ultrapure water. The filter and subsample was then dried at 60 °C and reweighed until a stable weight was achieved. Total daily mass flux (TMF) was then obtained by dividing the dry weight by the sampling time period.

For sediment POC and particulate organic nitrogen (PON) analysis, a subsample was freeze-dried and ground. Samples for POC analysis were acidified using 8% sulphurous acid to remove inorganic carbon and redried according to Verardo et al. (1990). Samples were then analysed using a Carlos Erba CHNS-O EA1108 Elemental Analyser with an analytical uncertainty of $\pm 1.3\%$ for PON ($n=5$) and $\pm 0.4\%$ for POC ($n=5$).

For sediment biogenic opal (defined here as $SiO_2 \cdot 0.4H_2O$, and hereafter referred to as SiO_2) measurements were carried out using a method adapted from Mortlock and Froelich (1989). Sediment subsamples were freeze-dried overnight, crushed and re-equilibrated with the atmosphere overnight at room temperature. 10% H_2O_2 was initially added to each subsample to remove organic matter, and 10% HCl then added after 30 min to remove carbonate. The subsamples were sonicated and then left for 30 min. Ultrapure water was then added, the samples centrifuged at 3000 rpm and the clear supernatant removed. The residual solid samples were then dried in an oven for 24 h.

To dissolve the biogenic opal, 40 ml of 2 M Na_2CO_3 solution was added to each dried subsample, mixed well, sonicated and placed in a water bath at 85 °C. The subsamples were mixed again at 2 and 4 h. After 5 h, the tube was removed and centrifuged for 5 min. Twenty milliliter of the clear supernatant was then stored for analysis.

For opal analysis, 100 μl of the supernatant was diluted with ultrapure water up to 10 ml, and 200 μl each of molybdate, citric acid and amino acid reagents solutions (Hach) were added in turn. Diluted supernatants were left 1–2 h and then analysed using a spectrophotometer set at 815 nm wavelength. Supernatant Si concentrations were calculated from the standard calibration curve, and percent biogenic Si calculated from the mass of the original dried subsample. Percent Si mass measured was then converted to percent opal according to percent opal $= 2.4 \times$ %Si.

Opal, POC and PON were obtained by multiplying TMF by the percentage of each constituent measured in the subsample measured on the elemental analyser. The percent lithogenic material in the sediment samples was not directly measured but calculated by difference according to Francois et al. (2002), with the assumption of no $CaCO_3$.

3. Results

All results are reported as day number relative to 1st January 2005 which represents day 1.

3.1. Light, water-column macronutrient profiles and nutrient deficit-derived primary production estimates

The seasonal cycle of PAR in Marguerite Bay shows extreme seasonal variation due to its location south of the Antarctic Circle, with constant daylight periods during summer. Surface PAR showed a daily irradiance typically of 10 mol photons $m^{-2}\,d^{-1}$ during the study period (Venables et al., In press).

In the deeper water ($\geq$200 m) of the RaTS and MT sites average concentrations of nitrate and silicate were similar (Figs. 2 and 3). At the RaTS and MT sites macronutrients showed depletion in the upper 100 m relative to deep water, which is assumed to arise from phytoplankton nutrient uptake in the upper 100 m. The average annual exportable primary production measurement from nutrient deficit-derived calculations, related to these macronutrient profiles, was 12.8 and 8.3 mol C $m^{-2}\,y^{-1}$ for the RaTS site and MT site, respectively (Table 3).

3.2. Upper water-column hydrography and macro- and trace nutrients at the RaTS site

In the period of this study, early spring NPI depths were ~35 m in the 2005/2006 season and ~10 m in the 2006/2007 season (Clarke et al., 2008). Upper-ocean mixed layer depth (MLD) at the RaTS site is detailed in Meredith et al. (2010) and is defined as the depth at which the water is 0.05 kg m^{-2} denser than that at the surface. Between January 2005 and April 2007 the RaTS site experienced a typical pattern of seasonal variability of MLD, with a shallow MLD normally between 1 and 10 m during early and midsummer. The MLD deepened to ~50 m during winter.

Table 5 shows the average concentrations of the upper water-column (0–15 m) macronutrients during the spring–summer 2005–2006 sampling period at the RaTS site. Macronutrient depletion occurred in the surface waters (0 m) during the bloom from day 369–416 (Average NO_3^-, SiO_2^- and PO_4^{2-} at 0 m of 3.6, 30.3 and 0.41 mmol m^{-3}; results not shown) relative to 15 m (Average NO_3^-, SiO_2^- and PO_4^{2-} at 0 m of 12.5, 52.5 and 0.74 mmol m^{-3}; results not shown). Silicate was usually present in high concentrations relative to the other macronutrients measured. In terms of nitrogenous compounds, nitrate was generally dominant, with ammonium and urea minor components. Phosphate and ammonium were at similar concentrations throughout the sampling period.

All macronutrients concentrations in the upper water-column were similar to those shown by Clarke et al. (2008). Clarke et al. (2008) presents monthly averages of the nutrient concentrations at 15 m depth for several years and therefore better represents the seasonal nutrient cycle at the RaTS site. TDFe showed an average of 22.2 μmol m^{-3} (Fig. 5) with the maximum concentration of TDFe occurring on day 369.

3.3. Carbon and nitrogen isotope uptake rates, and rate measurement-derived primary production estimates

The water-column integrated primary production derived from the ^{14}C uptake measurements was highly variable. These values ranged from 4.3 mmol C $m^{-2}\,d^{-1}$ (Day 416) to

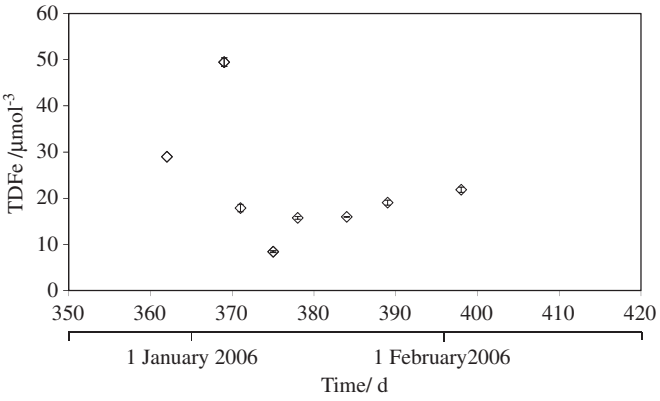

Fig. 5. Total dissolvable iron (TDFe) at 15 m at the RaTS site. Error bars show standard error (n=4). Day 365 is 1st January 2006.

Table 5
Average nutrient concentrations for upper water-column (0–15 m) at RaTS site (Range shown in brackets).

Date (dd/mm/yy)	Day number	Silicate/(mmol m^{-3})	Phosphate (mmol m^{-3})	Nitrate (mmol m^{-3})	Ammonium (mmol m^{-3})		Urea/ (mmol m^{-3})
28/12/05	362	36.6[a]	0.6[a]		10.6[a]	–	0.1[a]
04/01/06	369	49.9 (31.4–57.8)	0.8 (0.4–1.2)		16.0 (6.2–20.8)	0.6 (0.3–0.8)	0.2 (0.0–0.3)
06/01/06	371	48.5 (35.0–56.5)	0.5 (0.4–0.7)		8.9 (5.5–14.3)	0.3 (0.3–0.4)	0.3 (0.1–0.6)
10/01/06	375	39.5 (21.3–53.2)	0.4 (0.3–0.6)		3.8 (0.0–9.9)	0.3 (0.1–0.8)	0.2 (0.1–0.3)
13/01/06	378	40.0 (29.3–46.7)	0.2 (0.2–0.2)		3.9 (0.0–10.2)	0.4 (0.2–0.9)	0.6 (0.0–1.1)
19/01/06	384	47.1 (37.5–53.4)	0.4 (0.3–0.5)		6.0 (3.9–9.7)	0.3 (0.3–0.4)	0.5 (0.4–0.5)
24/01/06	389	49.7 (44.7–52.6)	0.7 (0.7–0.8)		9.6 (7.7–11.7)	0.8 (0.6–1.1)	0.1 (0.0–0.2)
30/01/06	395	37.6 (6.2–53.1)	0.6 (0.4–0.9)		8.3 (1.7–12.7)	1.5 (0.4–2.5)	0.2 (0.1–0.4)
02/02/06	398	24.3 (10.1–50.6)	0.7 (0.3–1.3)		4.1 (0.0–12.6)	0.8 (0.2–2.3)	0.4 (0.3–0.5)
13/02/06	409	47.6 (33.0–53.1)	0.5 (0.3–0.5)		11.8 (10.6–13.0)	0.9 (0.8–1.4)	0.2 (0.0–0.3)
20/02/06	416	33.0[a]	0.3[a]		8.5 (7.5–10.3)	0.5 (0.3–0.6)	0.3 (0.0–0.5)

[a] Sample taken at 15 m only.

593.2 mmol C m^{-2} d^{-1} (Day 371), with an average value of 266.5 mmol C m^{-2} d^{-1} for the sampling period (Fig. 4). The depth integrated N uptake rates showed an average total N uptake for the whole sampling season of 0.48 mmol N m^{-2} h^{-1}, with nitrate uptake always dominating total N uptake (Fig. 6). Average nitrate, ammonium and urea integrated uptake rates were 0.43, 0.08 and 0.02 mmol N m^{-2} h^{-1}, respectively. There were two distinct peaks in total N uptake due to high nitrate uptake on days 375 and 409 of 1.67 and 1.04 mmol N m^{-2} h^{-1}.

Exportable primary production, derived from ^{14}C and ^{15}N uptakes measurements, followed total primary productivity rates. Exportable primary production rates ranged from 3.6 mmol C m^{-2} d^{-1} (Day 416) to 523.9 mmol C m^{-2} d^{-1} (Day 371), with an average of 215.3 mmol C m^{-2} d^{-1} (Fig. 4).

3.4. Sediment trap flux and elemental composition

Dry mass flux showed consistent temporal patterns for both the RaTS and MT sites, with high flux periods in summer when upper water-column biomass (indicated by 15 m chl *a*) was highest (Fig. 7a). During the spring–summer period (1st November–1st April each year i.e., days 1–91, 305–455 and

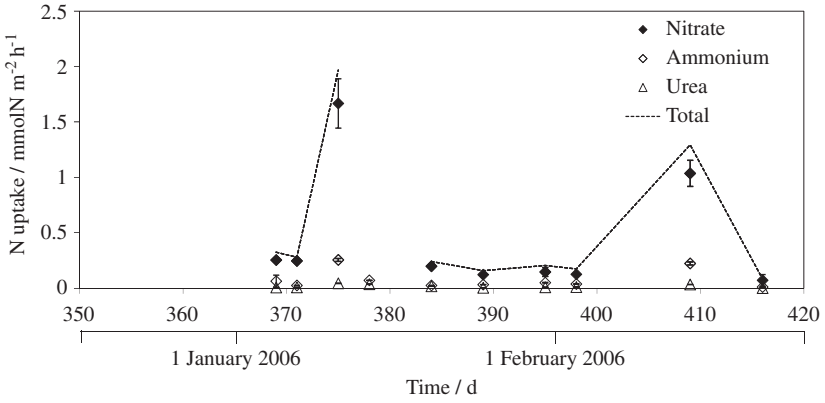

Fig. 6. Water-column integrated N uptake rates production to the depth of the Net Photocompensation Irradiance (NPI; see Table 4) at the RaTS site. Day 365 is 1st January 2006. Error bars show standard error ($n=3$). The gap in the 'Total' N uptake was due to the loss of nitrate uptake samples during analysis.

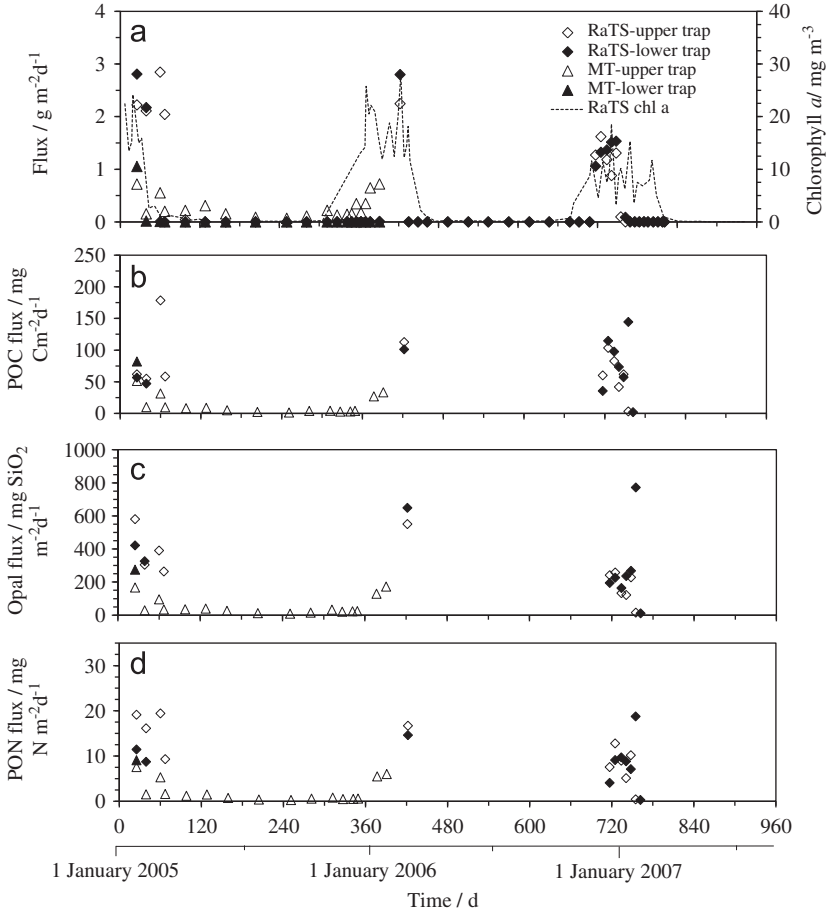

Fig. 7. (a) Water-column chlorophyll *a* concentration at 15 m at the RaTS site and sediment trap total dry mass flux, (b) sediment trap particulate organic carbon (POC) flux, (c) sediment trap biogenic opal (SiO_2) and (d) sediment trap particulate organic nitrogen (PON) flux to RaTS and MT sediment traps.

Table 6
Annual flux to all sediment traps for total dry mass flux, particulate organic carbon (POC), opal and particulate organic nitrogen (PON).

Trap/depth	Total dry mass flux ($g\,m^{-2}$)			POC ($g\,m^{-2}$)			Opal ($g\,m^{-2}$)			PON ($g\,m^{-2}$)			(%) lithogenic		
Year	2005[a]	2005–2006	2006–2007	2005[a]	2005–2006	2006–2007	2005[a]	2005–2006	2006–2007	2005[a]	2005–2006	2006–2007	2005[a]	2005–2006	2006–2007
Day number[b]	0–90	91–455	456–821	0–90	91–455	456–821	0–90	91–455	456–821	0–90	91–455	456–821	0–90	91–455	456–821
RaTS/upper[c]	158.59	30.67	46.57	5.07	1.47	2.61	25.44	7.15	7.26	1.03	0.22	0.33	77.6	67.1	73.2
Rats/lower[c]	84.98	36.69	78.05	1.77	1.32	3.86	12.75	8.43	13.36	0.34	0.19	0.42	80.8	69.8	73.0
MT/upper[d]	23.37	65.30	–	1.44	2.00	–	4.68	10.13	–	0.22	0.34	–	67.7	78.4	–
MT/lower[d]	15.19	0.19	–	1.15	–	–	3.85	–	–	0.13	–	–	59.5	–	–

[a] Sediment traps were not deployed for the whole spring–summer flux period in 2005 period for both MT and RaTS sites.
[b] Where day 1 is 1st January 2005.
[c] Since flux in sediment trap bottles during trap recovery were not used in results, there may be an underestimation of total annual flux in the 2005–2006 and 2006–2007 periods for RaTS site.
[d] Sediment traps were not deployed for the whole spring–summer flux period in 2005–2006 period for the MT site.

669–821) the flux for all traps ranged from 0.00 to 4.03 $g\,m^{-2}\,d^{-1}$. The average annual dry mass, POC, opal and PON fluxes for all traps (Table 6) was variable between years and depths for the same site. Overall, flux was consistently highest in the spring–summer period.

Flux was minimal in winter for the lower MT trap and both RaTS traps ($<0.02\ g\,m^{-2}\,d^{-1}$), albeit with flux to the MT upper trap decreasing at a slower rate during autumn/winter than for the RaTS traps. For the upper MT trap only, sample sizes were large enough to allow POC, PON and opal composition to be measured over an annual cycle (Fig. 7b–d). This higher winter flux to the MT upper trap relative to the RaTS upper trap may be due to its shallower deployment depth.

At the RaTS site, 2 full years of dry flux (1st April–31st March 2005–2006 and 2006–2007; i.e., days 91–455 and 456–821, respectively) are available. POC, opal and PON flux measurements were made during the spring and summer period (Fig. 7b–d) when flux was highest. The very low fluxes during the winter period mean that the combined spring and summer flux for POC, opal and PON are essentially equivalent to annual flux. Biogenic export was dominated by opal (Table 6). These results do however exclude the flux collected in the bottle open when the sediment traps were recovered as noted above.

For the MT sediment traps, total annual flux is shown for 2 years (Table 6). It should be noted that the flux measurements for '2005' period (Days 0–90) started during a high flux period and for 2005–2006 (Days 91–455) ended during a high flux period (Fig. 7a). The flux measurements for the MT site were therefore not for the whole of a 12 month period, and are therefore underestimates of total annual flux. The MT site showed variability of flux between years and depths as for the RaTS site, with similar export to the MT upper trap as for the RaTS site.

Data for the RaTS site (Fig. 8a–c) showed similar % POC, % opal and % PON in the upper trap (average 4.6%, 15.7% and 0.7%, respectively) to the lower trap (average 4.1%, 16.7% and 0.5%, respectively) during the higher flux period when sufficient sample was available to allow complete chemical analyses. At the MT upper trap, sufficient sample was available to allow chemical characterisation in the winter low flux period, and hence % POC, % opal and % PON was available for the whole of one annual cycle. For this trap % POC, % opal and % PON decreased from 4.2%, 18.3% and 0.7% in autumn/winter to, respectively to 3.0%, 14.3% and 0.5%, respectively in summer/spring period.

POC: opal, and POC: PON (Fig. 8d–e) were on average of 1.6 and 8.1, respectively for the upper RaTS trap and 1.5 and 9.3, respectively for the lower RaTS trap. For the MT site, the lower MT trap had only a single value each for POC: opal and POC: PON of 1.7 and 10.6, respectively. For the upper MT trap, POC: opal and POC: PON remained relatively constant throughout the year with an average of 1.2 and 7.1, respectively.

Lithogenic material was always dominant in trap material at both mooring sites, e.g., 60–81% (Table 6). Percent lithogenic material at the RaTS site was similar between upper and lower traps for all sampling events. Percent lithogenic material in the upper traps was similar at the MT and RaTS site, with the lowest percent lithogenic material in MT lower trap.

In summary, the RaTS site and MT site showed similar trends for particle flux, with a relatively temporally short summer high particle (and POC, opal and PON) flux period. The relative elemental composition was on average close to Redfield ratio values, i.e., ~1:1 POC:opal and ~6.6:1 POC:PON, in all traps at MT and RaTS site. The average percent composition of the material was similar between depths for the RaTS traps. The upper MT trap also showed that the particle flux in winter was associated with POC-, opal- and PON-poor, but lithogenic-rich, material relative to the summer input. The ratios of POC:opal and POC:PON in the upper MT trap remained relatively constant throughout the year, despite increased summer export of POC, opal and PON, since the relative amount of POC, opal and PON exported did not change significantly from winter to summer.

4. Discussion

4.1. Hydrography, macronutrient profiles, and upper water-column measurements at the RaTS site

At the RaTS site, the phytoplankton bloom typically starts in November (Clarke et al., 2008). At this time the mean NPI depth climbs above the mean MLD. The depth of NPI shows a strong seasonal cycle with deepest values in early spring (Oct/Nov), shoaling to values <5 m in winter (Clarke et al., 2008). For the rest of the summer the bulk of the phytoplankton biomass is at or below 15 m, which is below the mean values of both the NPI and MLD at this time (Clarke et al., 2008). The MLD is an important control on productivity and export (Clarke et al., 2008) although bloom magnitude and duration is the result of a complex interplay between light, mixing and the duration of sea-ice (Venables et al., In press).

Phytoplankton typically bloom at the RaTS site for approximately 75 days, with chl *a* concentrations generally between 10 and 20 $mg\,m^{-3}$ (Clarke et al., 2008). The years of this study were characterised by moderate periods of winter sea-ice and summer

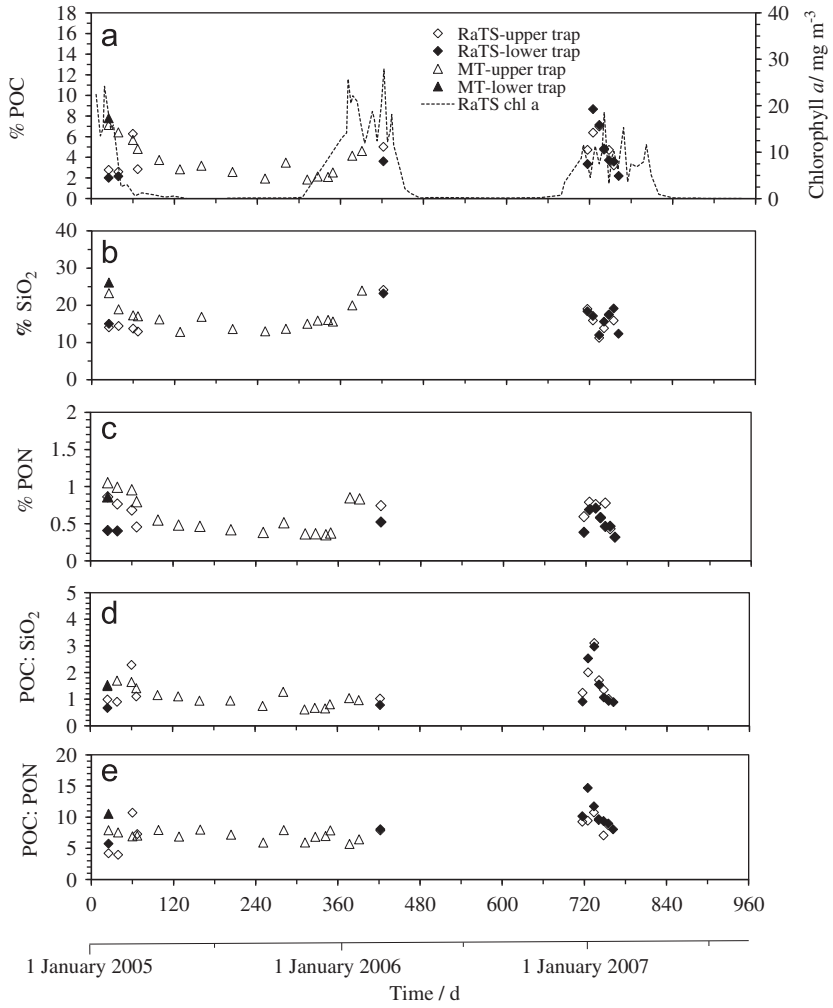

Fig. 8. (a) Water column chlorophyll *a* concentration at 15 m at the RaTS site and percent particulate organic carbon (POC), (b) percent opal, (c) percent particulate organic nitrogen (PON) of sediment trap flux, and (d) molar ratio of POC: opal and (e) molar ratio of POC: PON of sediment trap flux in RaTS and MT sediment traps.

blooms exceeding 20 mg chlorophyll *a* m^{-3} at peak (Fig. 7a). The bloom was dominated by diatoms (Annett et al., 2010) as generally found for southern coastal regions of the WAP (Huang et al., 2012). This highly productive short bloom was typical of coastal sites on the WAP (Ducklow et al., 2007).

Nutrient profiles at the RaTS and MT sites (Figs. 2 and 3) showed the impact of the phytoplankton growth as nutrient drawdown, but with significant residual concentrations throughout the surface waters. Nutrient concentrations below ~100 m were relatively constant, and high with depth. This vertical pattern was similar at both RaTS and MT sites, consistent with the earlier data and modelling for this region (Serebrennikova and Fanning, 2004; Serebrennikova et al., 2008). The nutrient drawdown extended below the depth of the NPI, reflecting mixing processes that continued throughout the growing season.

The TDFe concentrations, generally > 10 μmol m^{-3} (Fig. 5), were sufficient to support the primary production (Dulaiova et al., 2009) in agreement other studies on the WAP (Ardelan et al., 2010; Dulaiova et al., 2009). Dissolved Fe typically decreases with distance away from the continental shelf of the Antarctic Peninsula (de Jong et al., 2012), and may be limiting in other Antarctic coastal seas (Sedwick et al., 2000). TDFe availability in Marguerite Bay is expected to be high due to continued input resulting from glacial processes (Statham et al., 2008; Alderkamp et al., 2012).

The average spring and summer daily primary production rate of 267 mmol C m^{-2} d^{-1} (Fig. 4) at the RaTS site was similar to upper water-column primary production rates in summer for the coastal Palmer Long-Term Ecological Research (LTER) WAP site of ~220 mmol C m^{-2} d^{-1} (Moline and Prezelin, 1996). Primary production was however lower in the Bransfield Strait, also on the WAP, where an average value of 154 mmol C m^{-2} d^{-1} was recorded (Holm-Hansen and Mitchell, 1991). Summer primary production rates along the coastal WAP are significantly higher than for the Southern Ocean, with the latter having summer primary production rates of 10–18 mmol C m^2 d^{-1} (Gervais et al., 2002).

Water-column integrated N uptake rates at the RaTS site (Fig. 6) were comparable to the Southern Ocean and Antarctic coastal waters where uptake ranged from 2 to 42 mmol N m^{-2} d^{-1} (Savoye et al., 2004 and references therein). Nitrogen uptake measurements are often expressed in terms of the *f* ratio, in order to relate 'new' or 'exportable' primary production to total primary production (Eppley and Peterson, 1979). In this study water-column integrated nitrate uptake is assumed to represent 'new' production. The reduced forms of N, such as ammonium and urea, predominantly represent N recycled from heterotrophs. The *f* ratio ranged from 0.71 to 0.88 (Table 4) as a result of nitrate uptake dominating N uptake at the RaTS site throughout the bloom period (Fig. 6). The dominance of nitrate uptake at the RaTS site was in agreement with other studies in Antarctic shelf seas,

with average f ratios of 0.98 for the Weddell Sea in the late winter/early spring (Kristiansen et al., 1992) and 0.52 in summer (Savoye et al., 2004), and an f ratio of 0.64 in Bransfield Strait region for the developing spring bloom (Bode et al., 2002). In contrast to this study, Bode et al. (2002) showed regenerated production dominating after bloom development in the western Bransfield Strait.

There are problems associated with relating ^{15}N uptake measurements to new production. First, ammonium regeneration in the water column may lead to an underestimation of ammonium uptake (Eppley and Peterson, 1979). This regeneration has been shown to not be significant during a bloom in Antarctic coastal waters with similar f ratios to those presented in this study (Kristiansen et al., 1992). Ammonium regeneration is therefore not expected to significantly alter the f ratios reported here. Second, nitrification, i.e., microbially driven production of nitrate from ammonium, may result in overestimates of new production. This overestimate may occur since nitrate uptake resulting from nitrification will in effect be 'regenerated' production. Water-column nitrification rates of 6.0–8.9 nmol l^{-1} d^{-1} in the Ross Sea in summer (Olson, 1981), if applicable in Marguerite Bay, suggest nitrification may have a limited effect on new production estimates.

4.2. Sediment trap flux and composition

Sediment trap fluxes were highest in summer, consistent with trends in upper water-column chlorophyll and primary production measurements. Annual POC fluxes to the upper trap at the RaTS and MT site (Table 6) agreed with average annual flux measurements of 2.5 g C m^{-2} further north on the WAP shelf at the Palmer LTER mooring (deployed from 1992/1993 onwards; Ducklow et al., 2008). Daily POC fluxes at the moorings (Fig. 7b) agreed with daily fluxes in summer at the Palmer LTER mooring and the co-located 'FOODBANCS' mooring (Smith et al., 2008); the Palmer LTER mooring showed peak POC fluxes of between 100 and 1500 mg C m^{-2} d^{-1} and the deeper FOODBANC mooring showed POC fluxes of ~20–50 mg C m^{-2} d^{-1}. Mooring studies towards the northern end of the WAP in the Bransfield Strait also showed similar trends to Marguerite Bay, with maximum flux rates in summer of ~70 mg C m^{-2} d^{-1} (Palanques et al. 2002). In contrast to the low winter fluxes in this study and in Ducklow et al. (2008), a trap at the northern end of the peninsula, in a bay of Deception Island, showed high carbon flux rates of 12–120 mg C m^{-2} d^{-1} in the austral winter (Baldwin and Smith, 2003). These results illustrate the large differences in the seasonal patterns of flux along the length of the WAP, with consequences for carbon cycling and food supply to benthic detritivores (Smith et al., 2008).

Diatom bloom dominance (Annett et al., 2010) resulted in the high percentage of opal in the trap biogenic flux during summer (Fig. 7c). Annual fluxes of opal to the upper RaTS and upper MT traps (Table 6) were similar to the Ross Sea fluxes of ~110 mmol m^{-2} y^{-1} (Collier et al., 2000). Daily maximum summer opal fluxes in the Bransfield Strait of ~750 mg m^{-2} (Palanques et al., 2002), and in the eastern Weddell Sea of 826–901 mg m^{-2} (Isla et al., 2009) were also similar to daily fluxes at the RaTS and MT sites (Fig. 7c).

The POC: opal flux ratio (Fig. 8d) was higher than generally found in the open Southern Ocean (Fischer et al., 2002) and, although temporally variable, was similar between trap depths. This suggests close coupling of the Si and C cycles over the depth range considered here, although these cycles are decoupled on oceanic depth scales (Nelson et al., 1996). For the RaTS site, POC:PON, % POC, % opal and % PON (Fig. 8c–e) also showed similar trends between depths, as seen in POC:opal flux ratio, due to the coupling of biogeochemical cycles.

The average POC sediment composition of 4.4% for both mooring sites at peak flux periods was significantly lower than the >30% during summer in traps of the Palmer LTER mooring (Ducklow et al., 2008). This difference in POC flux between Marguerite Bay and Palmer LTER sites may be due to a combination of intense recycling of organic matter in the upper water-column in Marguerite Bay and higher lithogenic flux at our coastal sites than the offshore Palmer LTER site. At the Palmer LTER mooring there was intense recycling of the organic carbon flux, as at our mooring sites. Remineralisation however occurred deeper in the water column. This resulted in a % POC of ~2–12% in summer in deeper traps (Smith et al., 2008) compared to >30% in the shallow traps (Ducklow et al., 2008) at the Palmer LTER mooring site.

Since Ryder Bay is surrounded by glaciers and snowfields, with significant run-off during the summer melt (Meredith et al., 2010), lithogenic flux from glacial flour in meltwater is expected to have resulted in the high lithogenic flux at both MT and RaTS sites. The similarity of percent lithogenic composition of samples in upper and lower traps at the RaTS and MT site (Table 6) suggests that resuspension and horizontal near-bottom transport was not significant in the lower traps (cf. Collier et al. (2000)) relative to vertical processes. Although particulate inorganic carbon was not measured, it was expected to represent a small component of the flux since Palanques et al. (2002) showed that there was <2% total particulate inorganic C in a trap off the WAP. Trap samples in this study also had low foraminifera numbers (results not shown) and there are no recorded blooms of calcifying phytoplankton at the RaTS site (Annett et al., 2010).

The results presented for annual flux (Table 6) may however be an underestimate due to problems associated with the use of sediment traps, trap recovery and the period of trap deployment. Difficulties in accurately measuring sediment flux using tethered sediment traps are well documented (Asper, 1996; Buessler et al., 2007, 2010), with trapping problems associated with current velocities >12 cm s^{-1} (Baker et al., 1988). Marguerite Bay is characterised by generally low current speeds. Acoustic Doppler Current Profilers (ADCP) deployed on the same moorings as our sediment traps showed velocities of typically <10 cm s^{-1} in the upper 100–200 m, decreasing with depth (Wallace, 2008). These current speeds provide confidence in the efficiency of our sediment traps to collect flux, although we acknowledge that ADCPs do not profile velocity reliably to the surface.

The annual flux results presented for the RaTS site (Table 6) potentially underestimate total annual flux, since the flux contained in the trap bottle sampling during recovery was not used in the flux calculations. The trap bottle rotation was adjusted to limit sampling time loss to a maximum of 7 days. This represents ~10% of the 75 day bloom period (Clarke et al., 2008). Since flux is variable within this period we do not attempt to quantify this loss. The limited sampling period that was lost is not expected to invalidate our overall conclusions regarding the flux of organic matter and opal to the benthos at the RaTS site.

Unlike the sampling for 2005–2006 and 2006–2007 at the RaTS site, sampling for 2005 did not represent the whole spring–summer high flux period at either the RaTS or MT site (Fig. 7a). In addition the loss of the trap mooring in 2006 at the MT site prevented any full spring–summer high flux period being sampled (Fig. 7a). Annual flux at the RaTS site in 2005 and for the MT site in 2005 and 2005–2006 is therefore potentially significantly higher than presented in Table 6.

When sediment traps were recovered at the end of the austral winter, the trap funnel contained a significant amount of flux, i.e., more particulate matter than the trap bottle could contain. This

flux could not be quantified since it was lost on recovery of the sediment trap bottles. Visual inspection suggested a significant fine sediment fraction had been released by sea ice melt. Future sampling in this region should address this brief flux period.

4.3. Relating annual primary production measurements to sediment trap flux

Annual exportable primary production was derived using two independent methods; by nutrient deficit measurements and by uptake rate measurements. The nutrient deficit-derived calculations showed an average exportable primary production of 12.8 and 8.3 mol C m^{-2} y^{-1} for the RaTS site and MT site, respectively (Table 3). The rate measurement-derived annual exportable primary production was 16.0 mol C m^{-2} y^{-1} for the RaTS site (Table 3). Annual primary production from the rate measurements was higher than estimated by nutrient deficit measurements, most likely as a result of macronutrient supply into the upper water-column from deeper water during the summer period. The mechanism for this supply is expected to be a result of mixing from below (Wallace et al., 2008), through vertical diffusion, and via fluctuations in the depth of the mixed layer associated with variations in meteorological forcing (e.g., the passage of weather events) resulting in CDW entrainment (Meredith et al., 2004). Given the spatial and temporal variability in these environments, and limitations associated with each technique, the broad agreement between the two independent methods of exportable primary production is encouraging.

These annual primary production results (Table 3) are in agreement with annual primary production estimates derived from remote sensing data for the Palmer LTER for 1991–2006 (Ducklow et al., 2008) with an average 14.7 mol C m^{-2} y^{-1} flux, and the 9.1 mol C m^{-2} y^{-1} primary production calculated for the whole Antarctic continental shelf region (Arrigo et al., 2008b). Our exportable production estimates of 1.3–16.0 mol C m^{-2} y^{-1} (Table 3) also agree with a primary production estimate of 0.6–9.6 mol C m^{-2} y^{-1} derived from nutrient deficit calculations for Marguerite Bay and the adjacent continental margin (Serebrennikova and Fanning, 2004). Our daily exportable primary production measurements (Fig. 4) were, however, high compared to the daily rates of export production of 0–54 mmol C m^{-2} d^{-1} for the WAP region to the north of Marguerite Bay estimated by Huang et al. (2012). Huang et al. (2012) used the triple isotope composition of dissolved oxygen and this discrepancy between studies suggests that work is needed to reconcile these results.

The relationship between the exportable production in the upper water-column and the production exported to depth is critical in terms of predicting the potential for delivery of C to the seabed. The average annual POC flux to the upper sediment trap at the RaTS site for 2005–2006 and 2006–2007 was 2.04 g C m^{-2} (Table 6), i.e., flux for the years and the site where results for the whole high flux spring–summer period are available. This flux was as a result of an exportable annual primary production in the upper water-column of 192 and 154 g C m^{-2}, derived from rate measurements (Table 3) and the average of nutrient deficit measurements (Table 3), respectively at the RaTS site. Considered together, the relationship between these results implies an annual export to depth of only 1.1–1.3% of exportable primary production at the RaTS site. The interpretation of the significance of this difference between annual production and measured export flux to depth however needs to consider the various uncertainties and inevitable limitations of the methods used. The relatively good agreement between the two independent estimates of exportable flux provides some confidence in this estimate. As noted earlier, there are potential issues with our exported flux measurements. The relatively low current speeds in Marguerite Bay should minimise hydrodynamic bias in sediment trap collections but we cannot rule out such undersampling by our traps. There was additionally an unquantifiable underestimation of annual sampling by the sediment traps due to results from bottles sampling during trap recovery not being used. These issues together therefore imply that there may have been a greater flux of surface exportable production possible to deeper water than presented. However, even considering these caveats, it seems unlikely that these uncertainties could explain the very low percentage of the exportable flux intercepted by the sediment traps at depth. We therefore suggest Marguerite Bay can be characterised as 'high recycling, low export'.

This characterisation of Marguerite Bay is in agreement with other studies along the WAP. Ducklow et al. (2008) showed $<4\%$ of net primary production export between 1992 and 2007 for the Palmer-LTER region, and Isla et al. (2006) that suggested a flux of 0.6% of surface primary production to the benthos in the Bransfield Strait, WAP. Other Antarctic coastal regions also show low export; Smith and Dunbar (1998) showed an export of 2.6–3.0% of upper mixed layer 'new' primary production to a floating sediment trap at 250 m in the Ross Sea shelf during summer; Asper and Smith (1999) showed 2.3% C standing stock export in the same region.

The high recycling scenario in Marguerite Bay means that the particulate organic matter is expected to be subject to intensive remineralisation and grazing in the upper water-column (<200 m) during spring–summer. This is in agreement with Buessler et al. (2010) that showed recycling of $\sim$90% of the organic matter in the upper water-column in the WAP region. Although not directly measured, remineralisation may be indicated by the summer increase in ammonium concentrations (<0.3 up to ~3 μmol l^{-1}) at 15 m depth (Clarke et al., 2008). Grazing and secondary production by copepods (Ashjian et al., 2004), salps and krill (Ross et al., 2008) are potentially important in terms of driving this remineralisation. Secondary production in Marguerite Bay may turn out to be dominated by microzooplankton and small mesozooplankton, since their faecal pellets are mostly recycled in the upper water-column by microbial decomposition and coprophagy (Turner, 2002). In the Ross Sea mesozooplankton grazing has been shown to be important in limiting export (Gowing et al., 2001) but microzooplankton grazing rates were not significant in terms of altering export fluxes (Caron et al., 2000). More work is needed on the influence of recycling and grazing processes on particle export in Marguerite Bay.

Future export in Marguerite Bay may be influenced by changes in phytoplankton bloom species composition. Species dominance has shifted in other regions of the WAP from diatoms to cryptophytes (Moline et al., 2004), and Huang et al. (2012) showed greater export for cryptophyte-dominated communities than diatom-dominated communities on the WAP. This difference in export may result from different grazing mechanisms altering particle aggregation characteristics (Smith and Dunbar (1998); Arrigo et al., 1999; Asper and Smith, 1999).

Export may also change for the Marguerite Bay region as a consequence of climate change. Temperature change has already resulted in increasing air temperatures (King, 2003) linked to ice shelf collapse (Vaughan and Doake, 1996), and widespread retreat of glaciers (Cook et al., 2005) along the WAP. The continuation of the observed decadal trends in upper-ocean temperature and salinity (Meredith and King, 2005), and sea ice (e.g., Stammerjohn et al., 2008; Turner et al., 2009) will impact strongly on upper-ocean stratification and hence on the phasing and amplitude of the phytoplankton bloom (Venables et al., In press). On a local scale, the increasing temperatures (King, 1994) and the retreat of the George VI ice shelf in the south of

the Marguerite Bay (Lucchitta and Rosanova, 1998), will affect freshwater glacial input (Meredith et al., 2010). This may in turn affect physical and biogeochemical processes, including the timing and magnitude of the spring bloom, with potential consequences for export.

5. Conclusions

The RaTS site was shown to be highly productive in terms of both net and exportable primary production throughout the spring–summer phytoplankton bloom during the period 2005–2007. The agreement of annual exportable primary production estimates from rate measurement-derived and nutrient deficit-derived calculations suggests the RaTS site rate measurements were applicable to the wider Marguerite Bay. The measured export of ~1% of upper water-column exportable production to the sediment traps suggests intensive remineralisation of particulate organic matter in the upper 200 m of the water column. Marguerite Bay can therefore be characterised as 'high recycling, low export'.

The large long-term CO_2 sink in these regions, argued for by Arrigo et al. (2008a), requires export of organic matter to depths below winter mixing. This study demonstrates that this may not be the case, with implications for carbon sequestration and delivery of food to benthic fauna. This work is therefore in agreement with the global analysis of the biological pump by Lam et al. (2011) that showed that blooms dominated by large diatoms, as in Marguerite Bay, have low transfer efficiencies to deep water. An improved understanding of the role of heterotrophic processes is necessary before the relationship between upper water-column production and deep water flux can be quantitatively assessed and modelled. With rapid climate change occurring along the WAP shelf, the continuation of the RaTS sampling programme will be vital in helping our understanding and modelling of current and future export fluxes to the benthos.

Acknowledgements

The authors would like to thank the officers and crew of the RRS James Clark Ross. Kimberly Wright for assisting with the particulate carbon analysis, Dr. Martin Miller for organising logistics, Dan Combden, Jon Wynar and Rob MacLaclan at UKORS for mooring deployments. We would also especially like to thank the Marine Assistants at Rothera station's Bonner Laboratory; Paul Mann, Helen Rossetti and Andy Miller. This work was funded by NERC grant AFI 4-13 'Biogeochemical particle flux study in Marguerite Bay, Antarctica Peninsula'.

References

Alderkamp, A.-C., Mills, M.M., van Dijken, G.L., Laan, P., Thuróczy, G.-C., Gerringa, L.J.A., de Baar, H.J.W., Payne, C.D., Visser, R.J.W., Buma, A.G.J., Arrigo, K.R., 2012. Iron from melting glaciers fuels phytoplankton blooms in the Amundsen Sea (Southern Ocean): phytoplankton characteristics and productivity. Deep Sea Res. Part II 71-79, 32–48.

Almgren, T., Dyrssen, D., Fonselius, S., 1983. Determination of alkalinity and total carbonate. In: Grasshoff, K., Erhardt, M., Kremling, K. (Eds.), Methods of Seawater Analysis, second ed. Verlag Chemie, Weinheim, pp. 99–123.

Annett, A.L., Carson, D.S., Crosta, X., Clarke, A., Ganeshram, R.S., 2010. Seasonal progression of diatom assemblages in surface waters of Ryder Bay, Antarctica. Polar Biol. 1, 13–29.

Ardelan, M.V., Holm-Hansen, O., Hewes, C.D., Reiss, C.D., Silva, N.S., Dulaiova, H., Steinnes, E., Sakshaug, E., 2010. Natural iron enrichment around the Antarctic Peninsula in the Southern Ocean. Biogeosciences 7, 11–25.

Arrigo, K.R., Robinson, D.H., Worthen, D.L., Dunbar, R.B., DiTullio, G.R., VanWoert, M., Lizotte, M.P., 1999. Phytoplankton community structure and the drawdown of nutrients and CO_2 in the Southern Ocean. Science 283, 365–367.

Arrigo, K.R., van Dijken, G., Long., M., 2008a. Coastal Southern Ocean: a strong anthropogenic CO_2 sink. Geophys. Res. Lett. 35, L21602, http://dx.doi.org/10.1029/2008GL035624.

Arrigo, K.R., van Dijken, G.L., Bushinsky, S., 2008b. Primary production in the Southern Ocean, 1997–2006. J. Geophys. Res., 113.

Arrigo, K.R., Weiss, A.M., Smith Jr., W.O., 1998. Physical forcing of phytoplankton dynamics in the southwestern Ross Sea. J. Geophys. Res. 103, 1007–1021.

Ashjian, C.J., Rosenwaks, G.A., Wiebe, P.H., Davis, C.S., Gallager, S.M., Copley, N.J., Lawson, G.L., Alatalo, P., 2004. Distribution of zooplankton on the continental shelf off Marguerite Bay, Antarctic Peninsula, during Austral Fall and Winter, 2001. Deep Sea Res. Part II 51, 2073–2098.

Asper, V.L., 1996. Particle flux in the ocean: oceanographic tools. In: Ittekkot, V., Schafer, P.J., Honjo, S., Depetris, P.J. (Eds.), Particle Flux in the Ocean. Wiley, Chichester, pp. 71–84.

Asper, V.L., Smith Jr., W.O., 1999. Particle fluxes during austral spring and summer in the southern Ross Sea, Antarctica. J. Geophys. Res. 104, 5345–5359.

Baker, E.T., Milburn, H.B., Tennant, D.A., 1988. Field assessment of sediment trap efficiency under varying flow conditions. J. Mar. Res. 46, 573–592.

Baldwin, R.J., Smith, K.L., 2003. Temporal dynamics of particulate matter fluxes and sediment community response in Port Foster, Deception Island, Antarctica. Deep Sea Res. Part II 50, 1707–1725.

Barnes, D.K.A., Clarke, A., 1994. Seasonal variation in the feeding activity of four species of Antarctic bryozoan in relation to environmental factors. J. Exp. Mar. Biol. Ecol. 181, 117–133.

Beardsley, R.C., Limeburner, R., Owens, W.B., 2004. Drifter measurements of surface currents near Marguerite Bay on the western Antarctic Peninsula shelf during austral summer and fall, 2001 and 2002. Deep Sea Res. Part II 51, 1947–1964.

Bode, A., Castro, C.G., Doval, M.D., Varela, M., 2002. New and regenerated production and ammonium regeneration in the western Bransfield Strait region (Antarctica) during phytoplankton bloom conditions in summer. Deep Sea Res. Part I 49, 787–804.

Bowie, A.R., Achterberg, E.P., Mantoura, R.F.C., Worsfold, P.J., 1998. Determination of sub-nanomolar levels of iron in seawater using flow injection with chemiluminescence detection. Anal. Chim. Acta 361, 189–200.

Boyd, P.W., Robinson, C., Savidge, G., Williams, P.J., le, B., 1995. Water column and sea-ice production during austral spring in the Bellingshausen Sea. Deep Sea Res. Part II 42, 1177–1200.

Broecker, W., Peng, T.-H., 1982. Tracers in the Sea. Eldigio Press 690pp.

Buessler, K.O., Antia, A.N., Chen, M., Fowler, S.W., Gardner, W.D., Gustafsson, O., Harada, K., Michaels, A.F., Rutgers van der Loeff, M., Sarin, M., Steinberg, D.K., Trull, T., 2007. An assessment of the use of sediment traps for estimating upper ocean particle fluxes. J. Mar. Res. 65, 345–416.

Buessler, K.O., McDonnell, A.M.P., Schofield, O.M.E., Steinberg, D.K., Ducklow, H.W., 2010. High particle export over the continental shelf of the west Antarctic Peninsula. Geophys. Res. Lett. 37, L22606.

Caron, D.A., Dennett, M.R., Lonsdale, D.J., Moran, D.M., Shalapyonok, L., 2000. Microzooplankton herbivory in the Ross Sea, Antarctica. Deep Sea Res. Part II 47, 3249–3272.

Clarke, A., Meredith, M.P., Wallace, M.I., Brandon, M.A., Thomas, D.N., 2008. Seasonal and interannual variability in temperature, chlorophyll and macronutrients in northern Marguerite Bay, Antarctica. Deep Sea Res. Part II 55, 1988–2006.

Clarke, A., Murphy, E.J., Meredith, M.P., King, J.C., Peck, L.S., Barnes, D.K.A., Smith, R.C., 2007. Climate change and the marine ecosystem of the western Antarctic Peninsula. Philos. Trans. R. Soc. London, Ser. B 362, 149–166.

Collier, R., Dymond, J., Honjo, S., Manganini, S., Francois, R., Dunbar, R., 2000. The vertical flux of biogenic and lithogenic material in the Ross Sea: moored sediment trap observations 1996–1998. Deep Sea Res. Part II 47, 3491–3520.

Cook, A.J., Fox, A.J., Vaughan, D.G., Ferrigno, J.G., 2005. Retreating glacier fronts on the Antarctic Peninsula over the past half-century. Science 308, 541–544.

de Jong, J., Schoemann, V., Lannuzel, D., Croot, P., de Baar, H., Tison, J.-L., 2012. Natural iron fertilization of the Atlantic sector of the Southern Ocean by continental shelf sources of the Antarctic Peninsula. J. Geophys. Res. 117, G01029.

Ducklow, H.W., Baker, K., Martinson, D.G., Quentin, L.B., Ross, R.M., Smith, R.C., Stammerjohn, S.E., Vernet, M., Fraser, W., 2007. Marine ecosystems: the West Antarctic Peninsula. Philos. Trans. R. Soc. London, Ser. B 362, 67–94.

Ducklow, H.W., Erickson, M., Kelly, J., Montes-Hugo, M., Ribic, C.A., Smith, R.C., Stammerjohn, S.E., Karl, D.M., 2008. Particle export from the upper ocean over the continental shelf of the west Antarctic Peninsula: a long-term record, 1992–2007. Deep Sea Res. Part II 55, 2118–2131.

Dugdale, R.C., Goering, J.J., 1967. Uptake of new and regenerated forms of nitrogen in primary productivity. Limnol. Oceanogr. 12, 196–206.

Dulaiova, H., Ardelan, M.V., Hemderson, P.B., Charette, M.A., 2009. Shelf-derived iron inputs drive biological productivity in the southern Drake Passage. Global Biogeochem. Cycles 23, GB4014.

Eppley, R.W., Peterson, B.J., 1979. Particulate organic matter flux and planktonic new production in the deep ocean. Nature 282, 677–680.

Falkowski, P.G., Barber, R.T., Smetacek, V., 1998. Biogeochemical controls and feedbacks on ocean primary production. Science 281, 200–206.

Fischer, G., Gersonde, R., Wefer, G., 2002. Organic carbon, biogenic silica and diatom fluxes in the marginal winter sea-ice zone and in the polar front region: interannual variations and differences in composition. Deep Sea Res. Part II 49, 1721–1745.

Francois, R., Honjo, S., Krishfield, R., Manganini, S., 2002. Factors controlling the flux of organic carbon to the bathypelagic zone of the ocean. Global Biogeochem. Cycles 16, 1087, http://dx.doi.org/10.1029/2001GB001722.
Gervais, F., Riebesell, U., Gorbunov, M.Y., 2002. Changes in primary productivity and chlorophyll *a* in response to iron fertilization in the southern polar frontal zone. Limnol. Oceanogr. 47, 1324–1335.
Gowing, M.M., Garrison, D.L., Kunze, H.B., Winchell, C.J., 2001. Biological components of Ross Sea short-term particle fluxes in the austral summer of 1995–1996. Deep Sea Res. Part I 48, 2645–2671.
Holmes, R.M., Aminot, A., Kerouel, R., Hooker, B.A., Peterson, B.J., 1999. A simple and precise method for measuring ammonium in marine and fresh water ecosystems. Can. J. Fish. Aquat. Sci. 56, 1801–1808.
Holm-Hansen, O., Mitchell, B.G., 1991. Spatial and temporal distribution of phytoplankton and primary production in the western Bransfield Strait region. Deep Sea Res. Part I 38, 961–980.
Huang, K., Ducklow, H., Vernet, M., Cassar, N., Bender, M.L., 2012. Export production and its regulating factors in the West Antarctica Peninsula region of the Southern Ocean. Global Biogeochem. Cycles 26, GB2005, http://dx.doi.org/10.1029/2010GB004028.
Isla, E., Gerdes, D., Palanques, A., Teixido, N., Arntz, W., Puig, P., 2006. Relationships between Antarctic coastal and deep-sea particle fluxes: implications for the deep-sea benthos. Polar Biol. 29, 249–256.
Isla, E., Gerdes, D., Palanques, A., Gili, J.-M., Arntz, W.E., König-Langlo, G., 2009. Downward particle fluxes, wind and a phytoplankton bloom over a polar continental shelf: a stormy impulse for the biological pump. Mar. Geol. 259, 59–72.
JGOFS (1994). Report no. 19—Protocols for the Joint Global Ocean Flux Studies (JGOFS) Core Measurements. 210 pp.
Jickells, T.D., Liss, P.S., Broadgate, W., Turner, S., Kettle, A.J., Read, J., Baker, J., Cardenas, L.M., Carse, F., Hamren-Larssen, M., Spokes, L., Steinke, M., Thompson, A., Watson, A., Archer, S.D., Bellerby, R.G.J., Law, C.S., Nightingale, P.D., Liddicoat, M.I., Widdicombe, C.E., Bowie, A., Gilpin, L.C., Moncoiffé, G., Savidge, G., Preston, T., Hadziabdic, P., Frost, T., Upstill-Goddard, R., Pedrós-Alió, C., Simó, R., Jackson, A., Allen, A., DeGrandpre, M.D., 2008. A Lagrangian biogeochemical study of an eddy in the Northeast Atlantic. Prog. Oceanogr. 76, 366–398.
Karl, D., MichaeIs, A., Bergman, B., Capone, D., Carpenter, E., Letelier, R., Lipschlz, F., Paerl, H., Sigman, D., Stal, L., 2002. Dinitrogen fixation in the world's oceans. Biogeochemical 57, 47–98.
Karl, D.M., Tilbrook, B.D., Tien, G., 1991. Seasonal coupling of organic matter production and particle flux in the western Bransfield Strait, Antarctica. Deep Sea Res. Part I 38, 1097–1126.
Kim, D., Kim, D.-Y., Kim, Y.-J., Kang, Y.-C., Shim, J., 2004. Downward fluxes of biogenic material in Bransfield Strait, Antarctica. Antarctic. Science 16, 227–237.
King, J.C., 1994. Recent climate variability in the vicinity of the antarctic peninsula. Int. J. Climatol. 14, 357–369.
King, J.C., 2003. Antarctic Peninsula climate variability and its causes as revealed by analysis of historical records, in Antarctic Peninsula Climate Variability: historical and paleoenvironmental perpectives. In: Domack, E., Leventer, A., Burnett, A., Bindschadler, R., Convey, P., Kirby, M. (Eds.), Antarctic Research Series, 79. AGU, Washington D.C, pp. 17–30.
Kirkwood, D.S., 1996. Nutrients: Practical Notes on Their Determination in Seawater. ICES Techniques in Marine Environmental Sciences, no 17. International Council for the Exploration of the Seas, Copenhagen, 23 pp.
Klinck, J.M., Hofmann, E.E., Beardsley, R.C., Salihoglua, B., Howard, S., 2004. Water-mass properties and circulation on the west Antarctic Peninsula Continental Shelf in Austral Fall and Winter 2001. Deep Sea Res. Part II 51, 1925–1946.
Kristiansen, S., Syvertsen, E.E., Farbrot, T., 1992. Nitrogen uptake in the Weddell Sea during late winter and spring. Polar Biol. 12, 245–251.
Lam, P.J., Doney, S.C., Bishop, J.K.B., 2011. The dynamic ocean biological pump: insights from a global compilation of particulate organic carbon, $CaCO_3$, and opal concentrations from the mesopelagic. Global Biogeochem. Cycles 25, GB3009, http://dx.doi.org/10.1029/2010GB003868.
Lewis, M.R., Smith, J.C., 1983. A small volume, short incubation-time method for measurement of photosynthesis as a function of incident irradiance. Mar. Ecol. Prog. Ser. 13, 99–102.
Lewis, E., Wallace, D.W.R., 1998. Program Developed for CO_2 System Calculations. ORNL/CDIAC-105. Carbon Dioxide Information Analysis Center. Oak Ridge National Laboratory, U.S. Department of Energy, Oak Ridge, Tennessee.
Lucchitta, B.K., Rosanova., C.E., 1998. Retreat of northern margins of George VI and Wilkins Ice Shelves, Antarctic Peninsula. Ann. Glaciol. 7, 41–46.
Martin, J.H., Gordon., M., Fitzwater, S.E.. Iron in Antarctic Waters. Nature 345, 156–158.
Martinson, D.G., Stammerjohn, S.E., Iannuzzi, R.A., Smith, R.C., Vernet, M., 2008. Western Antarctic Peninsula physical oceanography and spatio–temporal variability. Deep Sea Res. Part II 55, 1964–1987.
Meredith, M.P., King, J.C., 2005. Rapid climate change in the ocean west of the Antarctic Peninsula during the second half of the 20th century. Geophys. Res. Lett., 32.
Meredith, M.P., Renfrew, I.A., Clarke, A., King, J.C., Brandon, M.A., 2004. Impact of the 1997/98 ENSO on upper ocean characteristics in Marguerite Bay, western Antarctic Peninsula. J. Geophys. Res. 109, C09013.
Meredith, M.P., Brandon, M.A., Wallace, M.I., Clarke, A., Leng, M.J., Renfrew, I.A., van Lipzig, N., King, J.C., 2008. Variability in the freshwater balance of northern Marguerite Bay, Antarctic Peninsula; results from $\delta^{18}O$. Deep Sea Res. Part II 55, 309–322.
Meredith, M.P., Wallace, M.I., Stammerjohn, S.E., Renfrew, I.A., Clarke, A., Venables, H.J., Shoosmith, D.R., Souster, T., Leng, M.J., 2010. Changes in the freshwater composition of the upper ocean west of the Antarctic Peninsula during the first decade of the twentieth century. Prog. Oceanogr. 87, 127–143.
Moffat, C., Beardsley, R.C., Owens, B., van Lipzig, N., 2008. A first description of the Antarctic Peninsula Coastal Current. Deep Sea Res. Part II 55, 277–293.
Moline, M.A., Claustre, H., Frazer, T.K., Schofield, O., Vernet, M., 2004. Alteration of the food web along the Antarctic Peninsula in response to a regional warming trend. Global Change Biol. 10, 1973–1980.
Moline, M.A., Prezelin, B.B., 1996. High resolution time-series data for 1991/1992 primary production and related parameters at a Palmer LTER coastal site: implications for modeling carbon fixation in the Southern Ocean. Polar Biol. 17, 39–53.
Montes-Hugo, M., Doney, S.C., Ducklow, H.W., Fraser, W., Martinson, D., Stammerjohn, S.E., Schofield, O., 2009. Recent changes in phytoplankton communities associated with rapid regional climate change along the Western Antarctic Peninsula. Science 323, 1470–1473.
Montes-Hugo, M.A., Vernet, M., Smith, R., Carder, K., 2008. Phytoplankton size-structure on the western shelf of the Antarctic Peninsula: a remote-sensing approach. Int. J. Remote Sens. 29, 801–829.
Mortlock, R.A., Froelich, P.N., 1989. A simple method for the rapid determination of biogenic opal in pelagic marine sediments. Deep Sea Res. Part A 36, 1415–1426.
Mulvenna, P.F., Savidge, G., 1992. A modified manual method for the determination of urea in seawater using diacetylmonoxime reagent. Estuarine Coastal Shelf Sci. 34, 429–438.
Nelson, D.M., DeMaster, D.J., Dunbar, R.B., Smith Jr., W.O., 1996. Cycling of organic carbon and biogenic silica in the Southern Ocean: estimates of water-column and sedimentary fluxes on the Ross Sea continental shelf. J. Geophys. Res. 101, 18,519–18,532.
Nelson, D.M., Smith Jr., W.O., 1991. Sverdrup revisited: critical depths, maximum chlorophyll levels, and the control of Southern Ocean productivity by irradiance-mixing regime. Limnol. Oceanogr. 36, 1650–1661.
Olson, R.J., 1981. ^{15}N tracer studies of the primary nitrite maximum. J. Mar. Res. 39, 203–226.
Palanques, A., Isla, E., Sanchez-Cabeza, J.A., Masque, P., 2002. Annual evolution of downward particle fluxes in the Western Bransfield Strait (Antarctica) during the FRUELA project. Deep Sea Res. Part II 49, 903–920.
Peterson, B.J., 1980. Aquatic primary productivity and the ^{14}C-CO_2 method: a history of the productivity problem. Annu. Rev. Ecol. Syst. 11, 359–385.
Platt, T., Gallegos, C.L., Harrison, W.G., 1980. Photoinhibition of photosynthesis in natural assemblages of marine phytoplankton. J. Mar. Res. 38, 687–701.
Pondaven, P., Ragueneau, O., Treguer, P., Hauvespre, A., Dezileau, L., Reyss, J.L., 2000. Resolving the 'opal paradox' in the Southern Ocean. Nature 405, 168–172.
Prezelin, B.B., Hofmann, E.E., Mengelt, C.C., Klinck, J.M., 2000. The linkage between upper circumpolar deep water (UCDW) and phytoplankton assemblages on the west Antarctic Peninsula continental shelf. J. Mar. Res. 58, 165–202.
Ross, R.M., Quetin, L.B., Martinson, D.G., Iannuzzi, R.A., Stammerjohn, S.E., Smith, R.C., 2008. Palmer LTER: patterns of distribution of five dominant zooplankton species in the epipelagic zone west of the Antarctic Peninsula, 1993–2004. Deep Sea Res. Part II 55, 2086–2105.
Savoye, N., Dehairs, F., Elskens, M., Cardinal, D., Kopczyaska, E., Trull, T.W., Wright, S., Baeyens, W., Griffiths, F.B., 2004. Regional variation of spring N-uptake and new production in the Southern Ocean. Geophys. Res. Lett., 31.
Sedwick, P.N., DiTullio, G.R., Mackey, D.J., 2000. Iron and manganese in the Ross Sea, Antarctica: seasonal iron limitation in Antarctic shelf waters. J. Geophys. Res. 105, 11,321–11,336.
Serebrennikova, Y.M., Fanning, K.A., 2004. Nutrients in the Southern Ocean GLOBEC region: variations, water circulation, and cycling. Deep Sea Res. Part II 51, 1981–2002.
Serebrennikova, Y., Fanning, K.A., Walsh, J.J., 2008. Modeling the nitrogen and carbon cycling in Marguerite Bay, Antarctica: annual variations in ammonium and net community production. Deep Sea Res. Part II 55, 393–411.
Smith Jr., W.O., Dunbar, R.B., 1998. The relationship between new production and vertical flux on the Ross Sea continental shelf. J. Mar. Syst. 17, 445–457.
Smith, R.C., Baker, K.S., Vernet, M., 1998. Seasonal and interannual variability of phytoplankton biomass west of the Antarctic Peninsula. J. Mar. Syst. 17, 229–243.
Smith, C.R., Mincks, S., DeMaster, D.J., 2008. The FOODBANCS project: introduction and sinking fluxes of organic carbon, chlorophyll-*a* and phytodetritus on the western Antarctic Peninsula. Deep Sea Res. Part II 55, 2404–2414.
Stammerjohn, S.E., Martinson, D.G., Smith, R.C., Yuan, X., Rind, D., 2008. Trends in Antarctic annual sea ice retreat and advance and their relation with ENSO and Southern Annular Variability. J. Geophys. Res. 113, C03S90, http://dx.doi.org/10.1029/2007JC004269.
Statham, P.J., Skidmore, M., Tranter, M., 2008. Inputs of glacially derived dissolved and colloidal iron to the coastal ocean and implications for primary productivity. Global Biogeochem. Cycles, 22.
Turner, D.R., 2002. Zooplankton fecal pellets, marine snow and sinking phytoplankton blooms. Aquat. Microb. Ecol. 27, 57–102.
Turner, J., Comiso, J.C., Marshall, G.J., Lachlan-Cope, T.A., Bracegirdle, T., Maksym, E., Meredith, M.P., Wang, Z., Orr, A., 2009. The non-annular atmospheric circulation change induced by stratospheric ozone depletion and its role in the recent increase in Antarctic sea ice extent. Geophys. Res. Lett. 36, L08502, http://dx.doi.org/10.1029/2009GL037524.

Vaughan, D.G., Doake, C.S.M., 1996. Recent atmospheric warming and retreat of ice shelves in the Antarctic Peninsula. Nature 379, 328–331.
Venables, H., Clarke, A.,. Meredith, M.P. Wintertime controls on summer stratification and productivity at the western Antarctic Peninsula. Limnol. Oceanogr. In press.
Verardo, D.J., Froelich, P.N., McIntyre, A., 1990. Determination of organic carbon and nitrogen in marine sediments using the Carlo Erba NA-1500 analyzer. Deep Sea Res. 37, 157–165.
Vernet, M., Martinson, D., Iannuzzi, R., Stammerjohn, S., Kozlowski, W., Sines, K., Smith, R., Garibotti, I., 2008. Primary production within the sea-ice zone west of the Antarctic Peninsula: I—Sea ice, summer mixed layer, and irradiance. Deep Sea Res. Part II 55, 2068–2085.
von Bodungen, B., Smetacek, V.S., Tilzer, M.M., Zeitzschel, B., 1986. Primary production and sedimentation during spring in the Antarctic Peninsula region. Deep Sea Res. Part A 33, 177–194.
Wallace, M.I., 2008. Ocean Circulation, Properties and Variability in Marguerite Bay, West Antarctic Peninsula. Ph.D. Thesis. The Open University, Milton Keynes, UK.
Wallace, M.I., Meredith, M.P., Brandon, M.A., Sherwin, T.J., Dale, A., Clarke, A., 2008. On the characteristics of internal tides and coastal upwelling behaviour in Marguerite Bay, west Antarctic Peninsula. Deep Sea Res. Part II 55, 2023–2040.
Walsby, A.E., 1997. Numerical integration of phytoplankton through depth and time in a water column. New Phytol. 136, 189–209.
Weston, K., Fernand, L., Mills, D.K., Delahunty, R., Brown, J., 2005. Primary production in the deep chlorophyll maximum of the central North Sea. J. Plankton Res. 27, 909–922.